Research article

Highly active antiretroviral therapy conjugated silver nanoparticle ameliorates testicular injury in type-2 diabetic rats

Samuel Oluwaseun Olojede [a,*], Sodiq Kolawole Lawal [a], Ayobami Dare [b], Roshila Moodley [c], Carmen Olivia Rennie [a], Edwin C.S. Naidu [a], Onyemaechi Okpara Azu [d]

[a] Discipline of Clinical Anatomy, School of Laboratory Medicine & Medical Sciences, Nelson R Mandela School of Medicine, University of KwaZulu-Natal, 719 Umbilo Road, Durban, South Africa
[b] Discipline of Physiology, School of Laboratory Medicine & Medical Sciences, College of Health Sciences, Westville Campus, University of KwaZulu-Natal, Durban, South Africa
[c] School of Chemistry and Physics, University of KwaZulu-Natal, Westville, Durban, South Africa
[d] Department of Human, Biological & Translational Medical Sciences, School of Medicine, University of Namibia, Hage Geingob Campus, Private, bag 13301, Namibia

ABSTRACT

Despite advances in managing human immunodeficiency virus (HIV) infection and success in the treatment prognosis using highly active antiretroviral therapy (HAART). The clinical efficacy of this regimen has been associated with increased adverse effects such as metabolic derangements and reproductive dysfunctions. These adverse effects necessitate a nanoparticle delivery vehicle like silver nanoparticles (AgNPs), a multi-functional drug delivery system, to transport the HAART to the viral reservoir site like testis.

This study was therefore designed to evaluate the effects of HAART loaded AgNPs (HAART-AgNPs) on testicular oxidative stress markers, an inflammatory biomarker, and histomorphology in a rat model of diabetes.

Thirty-six adult male Sprague-Dawley rats were randomly divided into two groups (n = 18) non-diabetic and fructose-streptozotocin (Frt-STZ) induced type 2 diabetes (T2DM). Thereafter, both groups were subdivided into three (n = 6) and treated with distilled water, HAART and HAART-AgNPs.

HAART-AgNPs caused a significant increase (p < 0.05) in catalase (23.43 ± 0.92) level vs diabetic control (16.95 ± 1.04). Also, HAART-AgNP caused a significant reduction (p < 0.05) in malondialdehyde, interleukin-6 and blood glucose levels (1.94 ± 0.06, 93.65 ± 3.6, 287.33 ± 22.85 respectively), compared to their respective diabetic control values (2.18 ± 0.12, 143.4 ± 9.2, 372.16 ± 23.16). Furthermore, HAART-AgNPs mitigated tubular atrophy, basement membrane thickening, interstitial distension, fibrous elemental distortion and peri-interstitial tissue alterations in the testis of diabetic rats.

The results from this study showed that administration of HAART-AgNPs to diabetic rats reduced testicular inflammation, improved glycaemic control, antioxidant status, and testicular histology. Therefore, conjugation of AgNP with HAART may cater for the reproductive dysfunction during the management of HIV infection.

1. Introduction

The advancement in combating human immunodeficiency virus (HIV) infection has led to the introduction of combination therapy, the highly active antiretroviral treatment (HAART). This combination therapy has brought about better therapeutic success, changing the course of this infection from a deadly to a chronic manageable condition (Cohen, D'Agostino, Tuzer and Torres, 2018; Iacob et al., 2017). Also, the introduction of HAART has remarkably enhanced the management, prognosis and quality of life in people living with HIV

infection, halt the emergence of opportunistic diseases, and enhances the immune system.

Unfortunately, the persistence of virus at the viral reservoir sites such as testis that presents blood-testis barrier (BTB) and viral rebound as a result of insufficient concentrations of antiretroviral drugs at these anatomical sanctuary sites has been described as one of the factors impeding complete eradication of HIV (Dahl, Josefsson and Palmer, 2010; Kis et al., 2010; Pace, Agosto, Graf and O'Doherty, 2011). Moreover, HAART requires continuous administration, which has been associated with adverse effects such as the development of drug resistance,

diabetes mellitus, unfavourable drug interactions and systemic drug toxicity (Fanta et al., 2020; Karpinski et al., 2016).

Reproductive dysfunction and metabolic disorders among other adverse effects of the HAART regimen are on the rise. A study has shown that type II diabetes mellitus (T2DM) promotes testicular damage with subsequent infertility (Long et al., 2018). Similarly, research has pointed at the generation of free radicals resulting from oxidative stress and elevation in the level of reactive oxygen species as primary causes of deoxyribonucleic acid (DNA) damage which subsequently impaired the sperm integrity in HIV patients under HAART (Savasi et al., 2018). Furthermore, an investigation has described the derangement in metabolic regulation due to the adverse effects of HAART and the consequences on inflammatory biomarkers such as interleukin 6 (IL-6) (Rose-John, 2018). Moreover, an increase in the plasma quantity of IL-6 was delineated as a biomarker for opportunistic diseases and death in patients under HAART (Rodger et al., 2009). Another investigation has reported excellent links between oxidative stress, IL-6 and reproductive dysfunction like infertility (Eggert-Kruse et al., 2001).

Therefore, to cater for the adverse effects of the HAART regimen in HIV patients, research attention has focused on employing nanoparticle delivery vehicles to circumvent the issue of biological barrier penetration and deliver HAART to anatomical sanctuary sites such as testis. Recently, drug delivery of HAART has received significant interest owing to the emerging field of nanotechnology (nanoparticles), which has been viewed to revolutionise the contemporary therapeutic modalities in HIV (Mahajan et al., 2012). Carbon-based, semiconductor, lipid-based, metallic, ceramic, quantum dots, porous materials and polymeric are the various classes of nanoparticles that have been identified and used in biomedical application, gene therapy, and drug delivery (Abdellah et al., 2020; Naidu et al., 2021).

Silver nanoparticles (AgNPs) among other metallic nanoparticles exhibit tuneable size, large surface area, enhanced bioavailability, targeted delivery, various shape, reactivity, sustained delivery, decrease in the emergence of drug resistance and antiviral properties (Dawadi et al., 2021; Gagliardi, 2017; Lee & Jun, 2019). A comprehensive review that examined the usage of metallic nanoparticles inferred that metallic nanoparticles such as silver NPs possess the ability to deliver antiretroviral agents due to their targeted delivery and decrease drug resistance development (Galdiero et al., 2011; Pradhan et al., 2021). Nanoparticles such as AgNP possesses sizes ranging from about 1 to 100 nm, a size like that of HIV, which makes it suitable for the various route of administration including intraperitoneal, intravenous, subcutaneous (Blanco et al., 2015; Patra et al., 2018), a size that may be responsible for the mode of delivering HAART. Moreover, the ability of AgNP to penetrate biological barriers including blood-testis-barrier and gain access to the anatomical sanctuary sites that harbours virus has been delineated (Blanco et al., 2015; Mzingwane and Tiemessen, 2017). Also, AgNP exhibits a large surface area to volume ratio, the property that is suitable for loading diverse therapeutic agents on their surface (Abbasi et al., 2016; Sinha et al., 2006). Based on antiviral activity, AgNP elicits this property through biding to glycoprotein 120 (gp120) on the cell surface, followed by blending, infecting and ultimately inhibition of cluster of differentiation 4 (CD4) (Lara et al., 2010b,c).

Unfortunately, till date, the unique characteristics of AgNPs are yet to be exploited to deliver HAART to the anatomical sanctuary sites and HIV latent reservoir sites. Hence, this study was designed to elucidate the interactions of HAART-AgNPs composite on the testis of a diabetic rat's model.

2. Materials and method

2.1. Statement on ethics and care for experimental animals

Ethical approval was received before the commencement of this investigation from the Animal and Research Ethics Committee (AREC) of the University of KwaZulu-Natal with the approval number AREC/043/

019D. The animal experimentation was carried out at the Biomedical Resource Unit (BRU) of the University of KwaZulu-Natal, Westville Campus. The animals received humane care following the Principle of Laboratory Animal Care of the University of KwaZulu-Natal standard approved guidelines.

2.2. Chemicals and highly active antiretroviral therapy

The Atripla, a combined highly active antiretroviral therapy (HAART) that contains Efavirenz (EFV, 600 mg), Emtricitabine (FTC, 200 mg) and Tenofovir disoproxil fumarate (TDF, 300 mg) was purchased from Dis-Chem pharmacy Ballito, South Africa. Streptozotocin (STZ), trisodium citrate, Sodium hydroxide and silver nitrate (AgNO$_3$) of analytical grade were purchased from Sigma-Aldrich Company, Johannesburg, South Africa.

2.3. Synthesis of AgNPs and conjugation of HAART-AgNP

The AgNP was prepared following the Turkevich method (Turkevich et al., 1951). The mass of 0.3 g of silver nitrate (AgNO$_3$) crystals was dissolved into a 500 mL volumetric flask marked with water to prepare a stock solution of 0.03 mol/dm^3. After that, the mass of 58.8 g of trisodium citrate was dissolved in a 50 mL volumetric flask and marked with 100 ml of distilled water to prepare 2 mol/dm^3. Briefly, 0.03 mol/dm^3 of AgNO$_3$ were mixed thoroughly with 2 mol/dm^3 of trisodium citrate and stirred for 5 min at 90 °C, at pH 10.5 of sodium hydroxide (NaOH) for 1 h 30 min. There was a change in the solution from colourless to amber yellow. The resultant AgNPs were cool at room temperature, 20 ml distil water was added to the samples then centrifuged at 12 000 rpm for 15 min, the same procedure was repeated and oven-dried at 40 °C, overnight. A mass of 15 g HAART was dissolved in 10 mL concentrated sodium hydroxide in a 50 mL volumetric flask and then topped up with diluted water (Lawal et al., 2021). The final concentration of the HAART solution was 1.05 M. The 50 mL HAART solution was mixed with 100 mL AgNPs aqueous solution. The mixture was under continuous stirring in ultra-sonication to ensure proper reaction of the components (HAART and AgNPs). The HAART silver nanoparticle (HAART-AgNPs) was centrifuged at 4,500 rpm at 40 °C, at 40 min to discrete the unincorporated drug. The supernatant was analysed using a UV spectrophotometer at a wavelength of 350 nm to calculate the quantity of unincorporated drug (W1) from the total amount of drug coupled with silver nanoparticle (W2).

The percentage of drug incorporation efficiency (% IE) was estimated by employing the below equation; Percentage incorporated efficiency (% IE) (Aboelwafa et al., 2010):

$$\% \, IE = \frac{HAARTW2 - HAARTW1}{HAARTW2} \, X \, 100\% \qquad \text{(Eq. 1)}$$

In Eq. (1) above, HAARTW2 is the total amount of highly active antiretroviral therapy loaded with silver nanoparticles, and HAARTW1 represents the quantity of unincorporated highly active antiretroviral therapy. The IE% for the HAART-AgNP synthesised was estimated to be 90.52 ± 0.5%.

2.4. Characterisation of AgNPs and HAART-AgNPs

The shape, size, morphology, functional group and elemental composition of the conjugates were examined. The absorption of the conjugates was measured by the Ultraviolet-visible (UV-Vis) spectroscopy (Shimadzu MultSpec-1501, Shimadzu Corporation, Tokyo, Japan). The size and morphology of the nanoparticles were examined by a high-resolution transmission electron microscope (HR-TEM, JEOL 2100, Japan) operated at a voltage of 200 kV, and field emission scanning electron microscope (FESEM, Carl Zeiss, Germany) operated at a voltage of 5 kV with energy dispersive x-ray (EDX, Aztec Analysis Software, England). The high-resolution transmission electron microscope (HTEM) and the field emission scanning electron microscope (SEM) confirmed

the shape and the size of the AgNPs. Also, the Fourier transform infrared (FTIR) spectroscopy (PerkinElmer Universal ATR spectrometer, USA) confirmed the conjugation of HAART to AgNPs while Energy-dispersive X-ray spectroscopy (EDX) confirmed the presence of elemental constituents of the HAART-AgNPs (Lawal et al., 2021).

2.5. Experimental design

In this study, a total of thirty-six adult male Sprague-Dawley rats weighing between 230-250 g were used. The experimental animals were housed in well ventilated plastic cages (3 rats per cage having dimensions of 52 cm long × 36 cm wide and 24 cm high with bedding of softwood shavings). The animals were maintained under standardised animal house conditions with temperature ranges from 23 to 25 °C; 12 h of natural light per day. The rats were fed with standard rat pellets from Meadow feeds, division of Astral Operations Limited, Durban, South Africa and given tap water ad libitum. Then the rats were randomly allotted to two (2) divisions, diabetic (n = 18) and non-diabetic n = 18).

2.6. Induction of type II diabetes mellitus

The rats allocated to the diabetic division received fructose and streptozotocin (STZ) (Frt-STZ) to induce type II diabetes mellitus (T2DM) by the model put forth by (Wilson and Islam, 2012). In this model, 10% fructose was added in drinking water ad-libitum for two (2) weeks to cause insulin resistance. After that, intraperitoneally induced the rats with 40 mg/kg body weight STZ freshly prepared in 0.1 M citrate buffer. Similarly, a volume of 0.1 M of citrate buffer was given to the non-diabetic rats. The diabetic model was characterised by hyperglycaemia through fasting blood sugar using Glucometer and strips (Acucheck$^{(R)}$, Boehringer-Mannheim, Germany). The rats with a blood glucose level of 200 mg/dL and above were regarded as diabetic and included in the diabetic division.

2.7. Animal grouping and administration of therapeutic agents

The non-diabetic and diabetic divisions were further allocated into three (3) groups, each with six (n = 6) rats as follows.

Group A represents non-diabetic control (NDC)- rats received 1 ml distilled water daily
Group B indicates non-diabetic HAART (NDH)—rats treated with 98.2 mg/kg/b. w/daily (p.o)
Group C represents non-diabetic nano HAART (NDNH)-rats received HAART-AgNPs (24.5 mg/kg/b. w/daily (i.p))
Group D indicates diabetic control (DC)– rats received 1 ml distilled water daily
Group E illustrates diabetic HAART (DH)—rats were treated with HAART (98.2 mg/kg/b. w daily (p.o))
Group F represents diabetic nano HAART (DNH)-rats received HAART-AgNPs (24.5 mg/kg/b. w/daily (i.p)).

A fixed-dose combination of highly active antiretroviral therapy (HAART) known as Atripla with Efavirenz, EFV (600 mg), Emtricitabine, FTC (200 mg) and Tenofovir disoproxil fumarate, TDF (300 mg) as active constituents in tablets form were used for this study. The tablets were crushed to powder, and adequate amounts weighed out following the recommended human doses. To calculate the animal dose from the recommended human dose, the formula; human equivalent dose =

$$HED \ (mg/kg) = \frac{Animal \ NOAEL \ (mg/kg) \ x \ Animal \ Weight \ (kg)}{Human \ weight \ (kg)^{1-0.67}}$$

(Eq. 2)

Eq. (2) above were used following the United States Food and Drug Administration recommendation (Nair and Jacob, 2016; Reigner and

Blesch, 2002). The rats in treatment groups were administered 53.6 mg/kg/day, 17.9 mg/kg/day and 26.8 mg/kg/day of Efavirenz, Emtricitabine, and Tenofovir disoproxil fumarate, respectively. The study ran for thirteen weeks, while the treatment ran for 56 days. Also, animals' distress, pain, and discomfort were taken care of by reducing the daily intraperitoneal administration in groups C and F to 6 out of 7 days. The rats were euthanised on day 57 by excessive Isoflurane inhalation, and blood samples were collected through the intracardiac puncture, and testicular tissues were excised for various analyses.

2.8. Bodyweight measurement

The body weights of the experimental animals were adequately measured and documented twice a week for the experiment period using a sensitive weighing balance (Metler, Greifensee, Switzerland).

2.9. Measurement of blood glucose level

The rats' blood glucose was checked by obtaining blood from the tail vein through pinprick and checked once a week throughout the study using a Glucometer (Acucheck$^{(R)}$, Boehringer-Mannheim, Germany).

2.10. Measurement of testicular weight

The weight of the testes was measured and recorded immediately after collection of a blood sample using a sensitive weighing balance (Metler, Greifensee, Switzerland). The relative testes weights were calculated for the testes using Eq. (3) below (Romano et al., 2010):

$$RTW = \frac{Testicular \ weight}{Total \ body \ weight} X100$$

(Eq. 3)

2.11. Tissue preparation for oxidative stress markers levels and IL-6

Briefly, 0.5 g of each harvested testes were homogenised in 5 mL sodium phosphate buffer with 1% Triton X-100 (50 mM; pH 7.5). Homogenates were then centrifuged for 10 min at 20,000 g (4 °C) in a Centrikon H-401 (Germany) centrifuge. Following centrifugation, the supernatants were collected, decanted into 2 mL Eppendorf tubes, labelled and preserved at - 80 °C until further analysis. The activities of the oxidative stress markers, Glutathione reductase (GSH) (Ellman, 1959), Malondialdehyde (MDA) (Ohkawa et al., 1979), Superoxide Dismutase (SOD) (Kakkar et al., 1984) and catalase (CAT) (Aebi, 1984), were analysed.

2.12. Estimation of testicular IL-6

The testicular sections were suspended in ice-cold 0.1 M phosphate buffer (pH 7.4) homogenised using a tissue homogeniser. The inflammatory cytokine concentration, IL-6, was determined from the testicular homogenate using an Enzyme-Linked Immunosorbent Assay kit (Catalogue no: E-EL-R0015) (ElabScience Biotechnology Co., Ltd., Houston, TX, USA) following the manufacturer's instructions strictly. Absorbance was measured using the microplate reader, SPECTRO star Nano spectrophotometer (BMG LABTECH, Ortenburg, LGBW, Germany).

2.13. Testicular histological analysis

The testicular tissues were dissected, weighed, and fixed immediately in Bouin's fluid for 24 h before tissue processing. The testes were sectioned at 4 μm thickness using Leica RM 2255 microtome, embedded in paraffin blocks, and stained with haematoxylin & Eosin (H&E), Periodic Acid Schiff (PAS) and Masson's Trichrome (MT). The stained slides of testis were cover-slipped using distyrene, plasticiser and xylene (DPX) mounting glue directly over the tissue section, ensuring that no air bubbles were trapped. After that, the slides were left overnight to dry for

examination under the light microscope. The sections were examined using a binocular Olympus microscope coupled with a digital image camera Nikon Eclipse 50i, Tokyo, Japan, to acquire the images.

2.14. Statistical analysis

The statistical analyses were performed on the variables using one-way analysis of variance (ANOVA), to determine the mean differences between the groups. Also, Tukey's multiple comparisons posthoc tests were carried out using Graph pad prism ® statistical software version 7.0. The results were expressed as mean ± standard deviation (SD) at a 95% confidence level (P < 0.05).

3. Results

3.1. Characterization of AgNP and HAART-AgNP

The characterization of the conjugated nanocomposites confirmed a spherical shaped AgNP with an average size between 19-32 nm. More-over, the presence of silver was confirmed in the HAART-AgNPs. Also, the successful conjugation of HAART to AgNP was confirmed with the presence of O–H, N–H, C–F, C–Cl, and C–N functional groups in HAART-AgNPs (Lawal et al., 2021).

3.2. Impact of HAART-AgNP on body weight, blood glucose level and relative testicular weight

The Frt-STZ diabetic control (DC) rats show a significant decrease in body weight (p < 0.05) when compared with non-diabetic control (NDC) rats. A significant increase (p < 0.05) in body weight was observed in diabetic rats treated with HAART when compared with diabetic control (DC) rats. More so, rats in the non-diabetic group treated with HAART showed a significant increase (p < 0.05) in body weight when compared with rats treated with HAART-AgNP (NDNH) and NDC. Frt-STZ-induced diabetic control (DC) rats showed a significant increase (p < 0.05) in blood glucose levels when compared with non-diabetic control (NDC) rats. Interestingly, Frt-STZ induced diabetic rats treated with HAART-AgNP (DNH) exhibited a significant reduction (p < 0.05) in blood glucose level when compared with diabetic control (DC) rats. In this investigation, a significant decrease (p < 0.05) in the relative testicular weights were noticed in the diabetic control (DC) compared with NDC rats (fig. 1a-c).
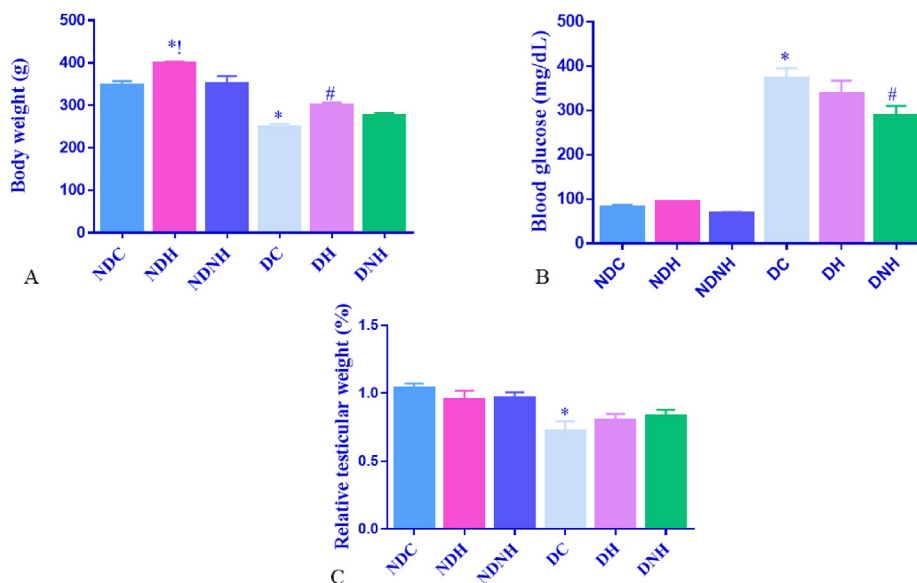
3.3. Impact of HAART-AgNP on antioxidant enzymes and malondialdehyde

As shown in figure 2a-d, Frt-STZ induced diabetic control (DC) rats had a significant reduction (p < 0.05) in the levels of GSH, SOD and CAT as well as a significant increase (p < 0.05) in MDA level vs with the non-diabetic control (NDC) rats. HAART-AgNPs increases catalase level vs DC and reduces MDA level in diabetic rats compared with DC and DH. However, administration of HAART to diabetic animals (DH) caused no significant change in oxidative stress biomarkers. Furthermore, chronic administration of HAART to non-diabetic rats caused a significant reduction (p < 0.05) in the level of SOD and CAT and increased MDA in non-diabetic rat vs NDC and NDNH.

3.4. Impact of HAART-AgNP on an inflammatory biomarker, IL-6

Figure 3 shows the concentration of IL-6 in the testicular homogenate of rats. There was a significant increase (p < 0.05) in the concentration of IL-6 in diabetic control rats (DC vs non-diabetic control (NDC) rats. However, a significant decrease (p < 0.05) in IL-6 was observed in diabetic rats treated with HAART-AgNPs (DNH) vs diabetic control rats (DC) and diabetic rats treated with HAART (DH). The concentration of IL-6 in diabetic rats administered with HAART (DH) was like that of diabetic control rats (DC). More so, administration of HAART-AgNP to non-diabetic rats caused no change in IL-6 concentration vs NC. In addition, there was an elevated IL-6 in non-diabetic rats treated with HAART compared with NDC and NDNH.

3.5. Impact of HAART-AgNP on the testicular histology

The H&E staining of the testicular section of non-diabetic control rats (NDC) revealed a normal structure of the seminiferous tubule with intact cellular components. Also, the lumen was populated with immotile spermatozoa with normal interstitial spaces. The H&E section of diabetic control (DC) rats was marked with substantial seminiferous tubule atrophy, widening interstitial spaces, sparse lumen. Tubular atrophy and interstitial space enlargement were evident in the H&E-stained sections of diabetic rats treated with HAART. Improvement in the testicular histological structures was observed in the section of diabetic rats treated with HAART-AgNPs.
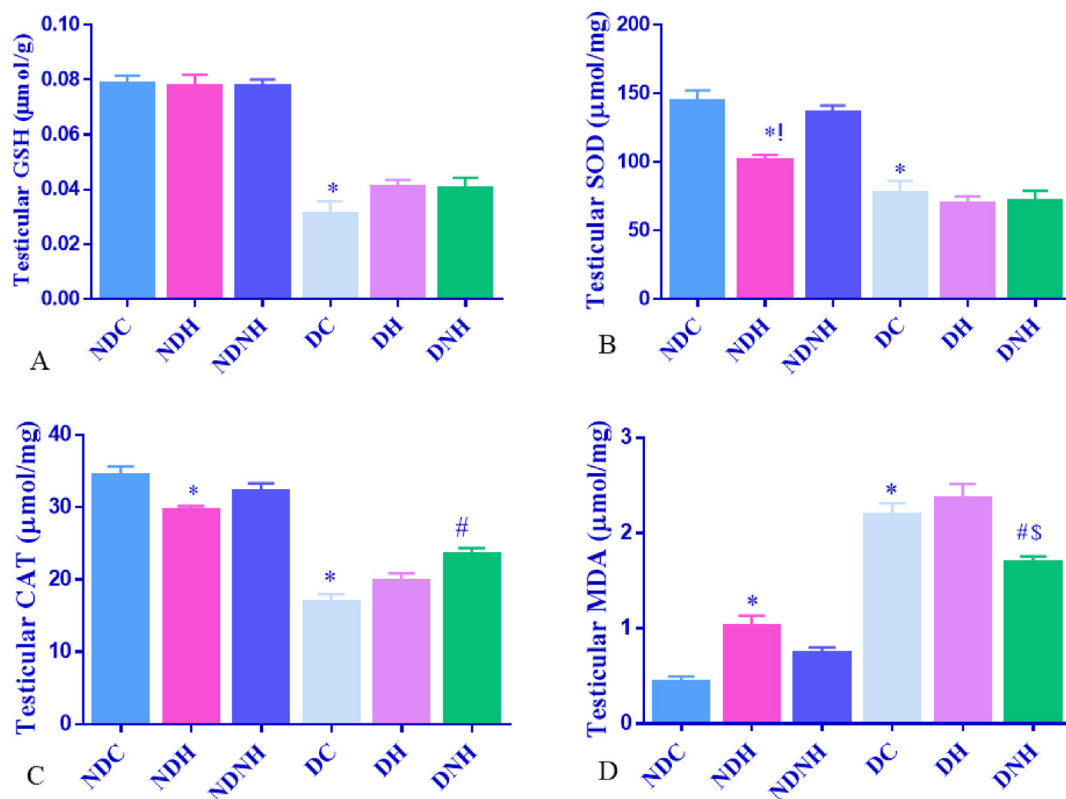

Figure 1. This figure illustrates the (A)-body weight, (B)-blood glucose and (C)-the relative testicular weight of the treated groups and control. Data are expressed as mean ± SEM of 6 rats per group, * compared with NDC; # vs DC; vs NDNH. One way ANOVA followed by Turkey's multiple comparison test was employed at p < 0.05.

Figure 2. Presents effect of various treatments on oxidative stress markers in diabetic and non-diabetic rats; (2A) Glutathione reductase (GSH); (2B) Superoxide dismutase (SOD); (2C) Catalase, (CAT) and (2D) Malondialdehyde (MDA) of the treated groups and control. NDC-Non-diabetic control; NDH-Non-diabetic HAART; NDNH-Non-diabetic nano HAART; DC-diabetic control; DH-Diabetic HAART; and DNH-Diabetic nano HAART. Data are expressed as mean ± SEM of 6 rats per group, * vs NDC; vs NDNH; # vs DC; $ vs DH. One way ANOVA followed by Turkey's multiple comparison test was employed at p < 0.05.
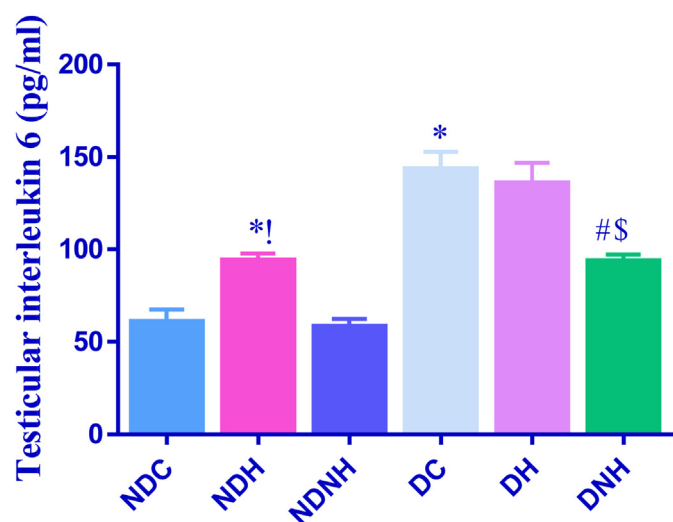

Figure 3. Depicts the testicular inflammatory cytokine, Interleukin 6 (IL-6), of the treated groups and control. * Compared with NDC; # vs DC, @ vs NDH, $ vs DH and ! vs NDNH. One way ANOVA followed by Turkey's multiple comparison test was employed at p < 0.05. NDC-Non-diabetic control; NDH-Non-diabetic HAART; NDNH-Non-diabetic nano HAART; DC-diabetic control; Diabetic HAART; and DNT-Diabetic nano HAART.

Also, testicular sections of non-diabetic rats treated with HAART showed slight tubular distension and few luminal spermatids. In addition, the section of non-diabetic rats administered with HAART-AgNP demonstrated a well-oriented seminiferous tubule characterised by a normal layout (Figure 4a).

In this study, the MT section of the non-diabetic control (NDC) rat showed usual, green-stained fibrous elements (collagen fibre) surrounding the testicular capsule without any distortions. The diabetic control rat showed an increase in collagen fibre with distorted orientation. However, the section of diabetic rats treated with HAART displayed an increase in collagen fibres marked with fenestration like DC. The MT-stained section of diabetic rats treated with HAART-AgNP showed a remarkable improvement in the cellular outlining and collagen fibres without any fibrous elemental distortions. Also, in DH, an increase in collagen fibre is like that of DC. Furthermore, there were normal MT-stained collagen fibres in the NDH and NDNH, but NDH has small fenestration (Yellow arrow) (Figure 4b).

The sections of non-diabetic control rats manifested normal PAS-stained cellular constituents and intact seminiferous tubule structure without any evidence of glycogen deposits. PAS-stained section of diabetic control rats revealed compromised integrity of the seminiferous tubule, weak PAS-stained peritubular interstitial tissues with depletion of Leydig cells, and thickened basement membrane. The extensively PAS-stained seminiferous tubular cells in diabetic rats treated with HAART were marked with tubular hypocellularity and a fewer distortion in the basement membrane. However, diabetic rats administered HAART-AgNP displayed normal PAS-stained peritubular interstitial tissue with normal Leydig cells without evidence of basement membrane detachment nor hypocellularity (Figure 4c). More so, the sections of NDH and NDNH demonstrates normal peritubular interstitial tissue positive PAS reaction, but few distortions in the basement membrane were noticed in NDH.

4. Discussion

Adverse effects such as insulin resistance, T2DM and reproductive dysfunction (Avari and Devendra, 2017; van Leeuwen et al., 2008) in HIV
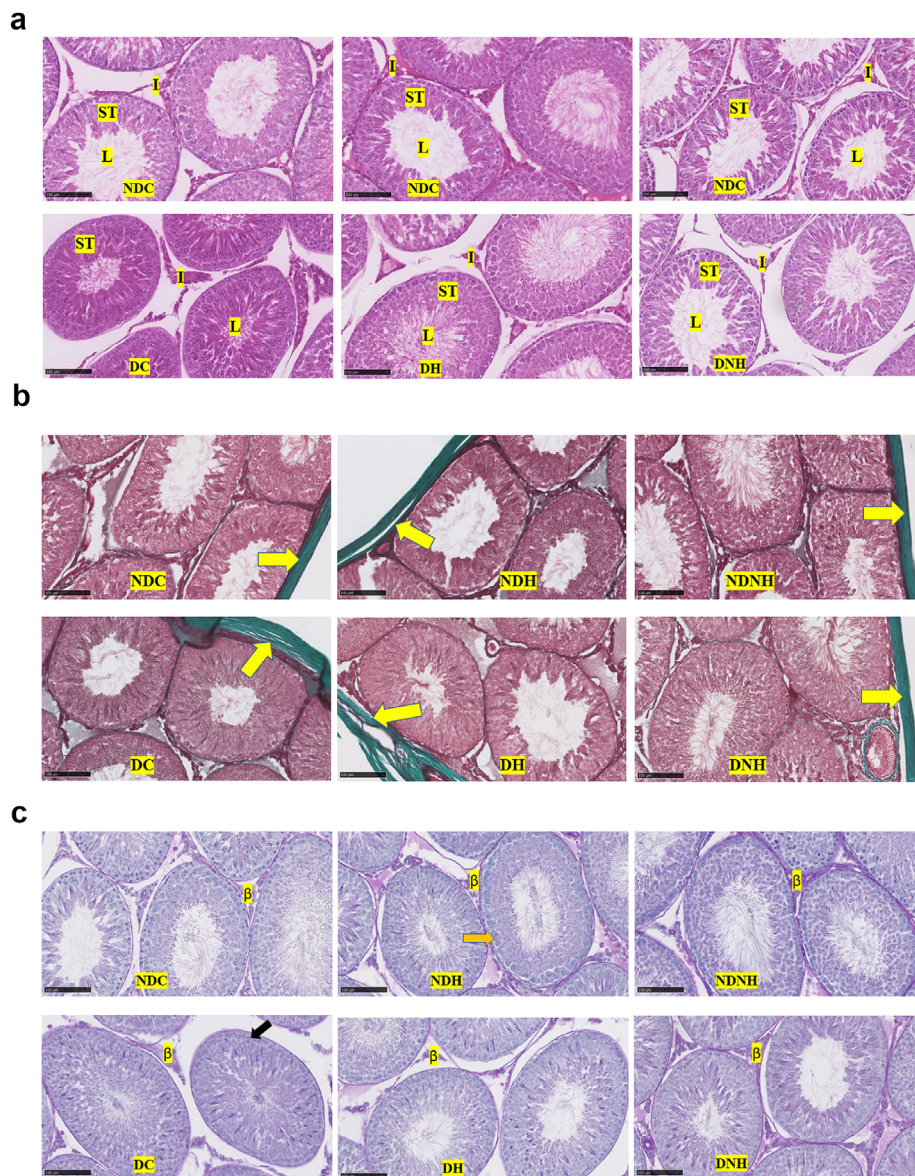
Figure 4. a: H&E micrographs of the testicular sections for the control and treatment groups (X 200). The NDC demonstrates the normal structure of seminiferous tubule (ST), interstitial spaces (I) with intact Leydig cells, intact cellular components and well-populated spermatozoa-filled lumen (L). DC shows widened interstitial spaces, shrunken ST and tubular atrophy with marked sparse spermatozoa in the lumen. The section of DH shows a distorted lumen and tubular atrophy with hypocellularity. However, the interstitial space of DNH contains normal Leydig cells with well-populated spermatozoa in the lumen. NDH has tubular distension, few distortions in the lumen, while NDNH exhibits H&E-stained like that of NDC. b: This figure depicts the Masson's Trichrome (MT) stained testicular sections of the control and treatment groups (MT) (X 200). The testicular capsule of the NDC shows normal MT-stained collagen fibres without any distortions (Orange arrow). The section of DC revealed increased collagen fibres with marked disorganised orientation (Orange arrow). However, there is a normal MT-stained collagen fibre in the capsule and surrounding the blood vessel in DNH. In addition, the section of DH shows an increase in collagen fibre similar to that of DC. There are normal MT-stained collagen fibres in the NDH and NDNH, but NDH has small fenestration (Yellow arrow). c: The PAS-stained micrographs of the control and treatment groups (X 200). The non-diabetic control (NDC) rat sections show normal ST basement membrane, with normal positive PAS-stained peritubular interstitial tissue (Yellow β) and Leydig cells. There is a weak peritubular interstitial tissue reaction with PAS in DC with disappearance in Leydig cells and thickened basement membrane (Black arrow). The section of DNH has peritubular interstitial normal PAS reaction with normal Leydig cells. Also, NDH and NDNH have normal peritubular interstitial tissue positive PAS reaction, but few distortions in the basement membrane were noticed in NDH (Yellow arrow).

infected persons necessitate a dire need for an effective delivery vehicle with little or no adverse effects. Moreover, an increase in biodistribution, improves solubility, and enhances stability with ultimate drug efficacy has been attributed to the use of AgNPs as drug delivery vehicle (Siddiqi et al., 2018). Given this reason, this study was undertaken to investigate the effects of the formulated HAART-AgNP on the testicular histology, inflammatory cytokine and oxidative stress markers in diabetic rats.

Characterization of the synthesized AgNPs was delineated as a method to assess its functional activities (Zhang et al., 2016). In this study, the synthesized AgNP and conjugated HAART-AgNPs were characterized to evaluate their functional characteristics (Lawal et al., 2021). The results of the synthesis revealed a spherical shape AgNP for the concentration of 1.5M with average size ranges between 19 and 32 nm. This finding conforms with a similar study that employed TSC as a reducing and stabilizing agent for the synthesis of AgNP (Yerragopu et al., 2020). Although, the toxicity profile of AgNPs have been documented but they were mostly dependent on the concentration, size, duration, shape and pH of the medium (Siddiqi et al., 2018). Previously, spherical shape AgNPs of sizes between 30 and 50 nm were not toxic to different HIV-1 isolates and cell culture (Lara et al., 2010a), and some biological specimens (Agnihotri et al., 2014; Jyoti et al., 2016).

Furthermore, the presence of major elemental constituents such as silver, chlorine, fluorine, carbon, oxygen, sodium and functional groups demonstrated successful conjugation of HAART to AgNP (Lawal et al., 2021), as supported by other studies (Agnihotri et al., 2014; Femi-Adepoju et al., 2019).

In this study, the increase in body weight observed with administration of HAART in diabetic and non-diabetic rats agrees with the previous study that evaluated the effects of HAART on the growth patterns in HIV infected children, which demonstrated its beneficial impacts on the body mass index, height and weight (Verweel et al., 2002). In another investigation, bodyweight gain at HAART initiation was described as composite events that may occur because of reversal in muscle wasting or build-up of fats caused by HAART (Carr, 2003).

Type II diabetes mellitus are marked by hyperinsulinemia, glucosuria, polydipsia, and hyperglycaemia (Hakim et al., 1997). Expectedly, an elevated blood glucose level observed in rats induced with DM using Frt-STZ in this study, confirming the successful induction of T2DM. Increased blood glucose levels have been reported as an aftermath of alteration in the β-cells functions and subsequent insufficient insulin secretion (Rossetti et al., 1990). Intriguingly, the evident decrease in blood glucose level noticed in diabetic rats treated with HAART-AgNPs,

suggesting an anti-diabetic activity of the spherical-shaped AgNP synthesized in this research. In a recent study, Saratale et al. (2017), demonstrated a synergistic and anti-diabetic effect of spherical shaped AgNP with an average size of 15 nm against alpha-amylase and alpha-glucosidase (Saratale et al., 2017). Other reports have shown inhibitory effects of AgNP on alpha-amylase and glucosidase, which in turn prevent catabolism of carbohydrates to monosaccharides, the primary cause of elevated blood sugar levels (Agarwal et al., 2021; Prabhu et al., 2018). The anti-diabetic impacts of AgNP, as reported, may cater for the reproductive adverse effects of HAART when loaded together.

Glutathione, superoxide dismutase, lipids, catalase and proteins are biosignatures of oxidative stress related to diabetes mellitus (Asmat et al., 2016). Oxidative stress has been delineated as a significant cause of different diabetic-related adverse effects (Ricci et al., 2009). Likewise, diabetic-associated oxidative stress alters normal reproductive physiology and induces testicular mitochondrial dysfunction (Ramalho-Santos et al., 2008). In this experiment, the reduced concentration of testicular antioxidant enzymes (GSH, SOD, CAT) and elevated the level of lipid peroxidation marker, MDA in diabetic rats indicate a compromise on the antioxidant defence system. Maritim et al. (2003) revealed that the formation of free radicals in diabetes mellitus by oxidation of glucose, glycation of protein and elevated lipid peroxidation causes an increase in insulin resistance, alteration in the antioxidant enzymes and damage to the cellular components (Maritim et al., 2003). The significant increase in testicular CAT and decrease in MDA in this study demonstrates some antioxidant activities of AgNP. Free radical scavenging properties of AgNP against radical scavengers of 2,2-diphenyl-1-picrylhydrazyl (DPPH), hydroxyl, nitric oxide, and superoxide with invitro deoxyribonucleic acid (DNA) protection were previously reported (Ramamurthy et al., 2013). AgNPs have received wide biomedical applications owing to their unique properties such as particle composition, rate of particle dissociation, large surface area, small size, surface chemistry and effectiveness in ion release (Zhang et al., 2016). These features suggest the antioxidant and free radical scavenger activity of AgNP. Surprisingly, no apparent changes were observed in antioxidant enzymes and lipid peroxidation of non-diabetic rats treated with HAART-AgNP, implying that the new formulation did not pose a deleterious implication on antioxidant enzymes. Furthermore, a remarkable reduction in testicular antioxidant enzymes, SOD and CAT, and elevation in MDA level in non-diabetic rats treated with HAART indicates damage to oxidative stress markers. This result aligns with a recent study that detailed a reduction in the quantity of testicular antioxidant enzymes (GSH, SOD, CAT) and an elevated amount of testicular lipid peroxidation in lean and obese rats treated with HAART (Oyeyipo et al., 2018). These findings taken together, reflect the detrimental effects of HAART on the testicular antioxidant defence system with subsequent testicular mitochondrial damage. Results of assessments on some semen parameters of HIV infected individuals placed on HAART has shown that these drugs are toxic to the mitochondrion, suggesting the mitochondrion as the main target of the HAART (van Leeuwen et al., 2008). Consequently, weakened testicular antioxidant activities have severe implications on reproductive indices.

IL-6 and other pro-inflammatory cytokines found in the seminal plasma of humans are essential indicators of reproductive system inflammation (Pilatz et al., 2013). Besides, IL-6 plays a crucial role in maintaining the reproductive processes, like developing spermatogenic cells and regulating the Sertoli cell (Hedger and Meinhardt, 2003). Most recently, an increase in the concentration of inflammatory markers, a subsequent increase in insulin resistance and the development of type II diabetes mellitus was delineated (Bashir et al., 2020). An increase in the level of IL-6 observed in diabetic rats suggest an inflammatory process. This finding augments a similar investigation that described elevated IL-6 expression and other inflammatory biomarkers in the testicular tissue of diabetic rats (Kolb and Mandrup-Poulsen, 2005; Rashid and Sil, 2015). Moreover, a significant decrease in the testicular IL-6

concentration in diabetic rats treated with HAART-AgNP may be ascribed to the anti-inflammatory effect of small-sized, spherical-shaped AgNPs. Recently, anti-inflammatory activities of silver-polyvinyl pyrrolidone (Ag-PVP) nanoparticles in a mouse infected with C. trachomatis was reported (Yilma et al., 2013). Previous studies have shown that AgNPs of low concentration were non-toxic to the human body, and it exhibits a wide range of antimicrobial and antiviral properties (Baker et al., 2005; Lara et al., 2010b,c). Furthermore, an increase in IL-6 concentration in diabetic rats treated with HAART indicates that HAART could not inhibit inflammatory cytokine in diabetic conditions. Also, this research revealed no changes in the testicular IL-6 expressions in non-diabetic rats treated with HAART-AgNPs. More so, non-diabetic rats treated with HAART exhibited a significant elevation in the level of IL-6. A cohort study of 3,695 non-diabetic people placed on HAART reported an increase in IL-6 level and subsequent development of diabetes in 137 patients (Dooko et al., 2014). This finding indicates that elevated IL-6 contributes to the pathogenesis of DM. In contrast to the result of this study, Osuji and co-workers (2018) documented no significant changes in the serum IL-6 concentration among HIV-infected and HIV seronegative patients after one year of HAART administration (Osuji et al., 2018). The discrepancy may be due to the duration, tissue specification and HAART cocktail used in both studies.

Histopathology has been described as a highly dependable tool to diagnose deleterious impacts or perturbations in male reproductive organs (Creasy, 2001; Lanning et al., 2002). In this regard, H&E, MT and PAS were employed to determine any alterations in testicular indices. The tubular atrophy, distortion in cellular outlining, increase in collagen fibre, weakly stained peritubular interstitial tissue, thickened basement membrane, and distension of tubular lumen observed in diabetic control rats suggested testicular damage. This result agrees with the previous finding that documented abnormal morphology of seminiferous tubules marked with distorted epithelium in diabetic rats (Ricci et al., 2009). Moreover, Ismail et al. (2017) reported an increase in collagen fibres with several distortions in diabetic rats, augmenting this present study's findings (Ismail et al., 2017). It is worthy to note that the administration of HAART-AgNP in diabetic rats improved the testicular histological architecture that was marked with tubular atrophy and interstitial distension. Notably, tubular atrophy, hypocellularity, few fenestrations in the collagen fibre and thickened basement membrane noticed in diabetic rats treated with HAART indicates that administration of HAART exacerbates the testicular histological alterations in diabetic rats. A similar experiment in diabetic rats treated with HAART revealed histological alterations in the testicular section (Olasile et al., 2018), indicating that administration of HAART may worsen the diabetic condition.

Interestingly, it was observed from this study that treatment with HAART-AgNP in non-diabetic exhibited no deleterious effects on the testicular histology, suggesting that the size of the AgNP used in this study was not toxic to the testicular histological architecture. Fathi et al. (2019) revealed no testicular histology and indices alterations among rats treated with 30 mg/kg AgNP. Their study showed morphological and histological distortions with 300 mg/kg of AgNP (Fathi et al., 2019). Their finding and this taken together suggests that detrimental impacts of AgNP are dose-dependent. Furthermore, some degree of morphological changes in the seminiferous tubule, interstitial spaces, and mild distension of the lumen noticed in non-diabetic treated with HAART suggested a detrimental effect of HAART in non-diabetic rats. A similar study on experimental rats have ascribed administration of a fixed-dose combination of HAART containing Tenofovir/Emtricitabine and Efavirenz to an adverse effect observed in the testicular histology and physiology (Adana, 2018), augmenting the result of this present research. Also, Ogedengbe et al. (2016) reported derangements in the testicular histology, with ST's apparent thickened basement membrane in a HAART treatment regimen containing Zidovudine, Lamivudine, and Nevirapine cocktail (Ogedengbe et al., 2016).

5. Conclusion

This study has demonstrated the beneficial impact of HAART-AgNP on blood glucose level (372.16 ± 23.16 vs 287.33 ± 22.85), testicular antioxidant enzymes, GSH (0.040 ± 0.0036 vs 0.030 ± 0.0048), catalase (23.43 ± 0.92 vs 16.95 ± 1.04), and MDA (2.18 ± 0.12 vs 1.94 ± 0.06), anti-inflammatory response, IL-6 (143.4 ± 9.2 vs 93.65 ± 3.6), and alleviated structural derangements (tubular atrophy, basement membrane thickening, interstitial distension, fibrous elemental distortion and peri-interstitial tissue alterations) in the testis of diabetic rats. In addition, the result of this investigation has revealed that administration of HAART in diabetic rats aggravate the diabetic condition. Hence, loading HAART with AgNP may cater for DM and reproductive dysfunction in the management of HIV infection by exploiting its antiviral and other features.

Declarations

Author contribution statement

Samuel Oluwaseun Olojede; Sodiq Kolawole Lawal: Conceived and designed the experiments; Performed the experiments; Analyzed and interpreted the data; Wrote the paper.

Ayobami Dare: Performed the experiments; Analyzed and interpreted the data; Contributed reagents, materials, analysis tools or data; Wrote the paper.

Roshila Moodley: Performed the experiments; Analyzed and interpreted the data.

Carmen Olivia Rennie: Conceived and designed the experiments; Analyzed and interpreted the data; Contributed reagents, materials, analysis tools or data; Wrote the paper.

Edwin C.S. Naidu: Conceived and designed the experiments; Analyzed and interpreted the data.

Onyemaechi Okpara Azu: Analyzed and interpreted the data; Contributed reagents, materials, analysis tools or data.

Data availability statement

Data included in article/supplementary material/referenced in the article.

Declaration of interests statement

The authors declare no conflict of interest.

Additional information

No additional information is available for this paper.

References

Abbasi, Elham, Milani, Morteza, Aval, Fekri, Sedigheh, Kouhi, Mohammad, Akbarzadeh, Abolfazl, Nasrabadi, Tayefi, Hamid, Nejati-Koshki, Kazem, 2016. Silver nanoparticles: synthesis methods, bio-applications and properties. Crit. Rev. Microbiol. 42 (2), 173–180.

Abdellah, Ahmed R., Abdelhamid, Nasser, Hani, El-Adasy, Abu-Bakr, A.A.M., Atalla, Ahmed A., Aly, Kamal I., 2020. One-pot synthesis of hierarchical porous covalent organic frameworks and two-dimensional nanomaterials for selective removal of anionic dyes. J. Environ. Chem. Eng. 8 (5), 104054.

Aboelwafa, Ahmed A., El-Setouhy, Ahmed, Doaa, Elmeshad, Aliaa Nabil, 2010. Comparative study on the effects of some polyoxyethylene alkyl ether and sorbitan fatty acid ester surfactants on the performance of transdermal carvedilol proniosomal gel using experimental design. AAPS PharmSciTech 11 (4), 1591–1602.

Adana M, Yetunde, 2018. Testicular Morphological and Biochemical Perturbations in Experimental Animals under Antiretroviral Therapy and the Role of Naringenin, a Bioactive Flavonoid. PhD Desertation.

Aebi, Hugo, 1984. Catalase in vitro. Methods Enzymol. 105, 121–126.

Agarwal, Happy, Kumar, S Venkat, Rajeshkumar, S., 2021. Antidiabetic effect of silver nanoparticles synthesized using lemongrass (Cymbopogon Citratus) through conventional heating and microwave irradiation approach. J. Microbiol. Biotechnol. Food Sci. 2021, 371–376.

Agnihotri, Shekhar, Mukherji, Soumyo, Mukherji, Suparna, 2014. Size-controlled silver nanoparticles synthesized over the range 5–100 nm using the same protocol and their antibacterial efficacy. RSC Adv. 4 (8), 3974–3983.

Asmat, Ullah, Abad, Khan, Ismail, Khan, 2016. Diabetes mellitus and oxidative stress—a concise review. Saudi Pharmaceut. J. 24 (5), 547–553.

Avari, Devendra, S., 2017. Human immunodeficiency virus and type 2 diabetes. Lond. J. Prim. Care 9 (3), 38–42.

Baker, C., Pradhan, A., Pakstis, L., Pochan, Darrin J., Shah, S Ismat, 2005. Synthesis and antibacterial properties of silver nanoparticles. J. Nanosci. Nanotechnol. 5 (2), 244–249.

Bashir, Haamid, Bhat, Showkat Ahmad, Sabhiya, Majid, Rabia, Hamid, Koul, Rakesh K., Rehman, Muneeb, U., Masood, Akbar, 2020. Role of inflammatory mediators (TNF-α, IL-6, CRP), biochemical and hematological parameters in type 2 diabetes mellitus patients of Kashmir, India. Med. J. Islam. Repub. Iran 34, 5.

Blanco, Elvin, Shen, Haifa, Ferrari, Mauro, 2015. Principles of nanoparticle design for overcoming biological barriers to drug delivery. Nat. Biotechnol. 33 (9), 941–951.

Carr, Andrew., 2003. HIV lipodystrophy: risk factors, pathogenesis, diagnosis and management. AIDS 17, S141–S148.

Cohen, D'Agostino, Luca, Tuzer, Ferit, Torres, Claudio, 2018. HIV antiretroviral therapy drugs induce premature senescence and altered physiology in HUVECs. Mechan. Ageing Dev. 175, 74–82.

Creasy, Dianne M., 2001. Pathogenesis of male reproductive toxicity. Toxicol. Pathol. 29 (1), 64–76.

Dahl Josefsson, Lina, Palmer, Sarah., 2010. HIV reservoirs, latency, and reactivation: prospects for eradication. Antivir. Res. 85 (1), 286–294.

Dawadi, Sonika, Katuwal, Gupta, Saurav, Lamichhane, Aakash, Uttam, Thapa, Ranjita Jaisi, Shankar, Parajuli, Niranjan, 2021. Current research on silver nanoparticles: synthesis, characterization, and applications. J. Nanomater. 2021.

Dooko, Claude Béténé, A., De Wit, Stephane, Neuhaus, Jacqueline, Palfreeman, Adrian, Pepe, Rosalie, Pankow, James, S., Neaton, James D., 2014. Interleukin-6, high sensitivity C-reactive protein, and the development of type 2 diabetes among HIV positive patients taking antiretroviral therapy. J. Acquir. Immune Defic. Syndr. 67 (5), 538 (1999).

Eggert-Kruse, Waltraud, Boit, Ruxandra, Rohr, Gerhard, Aufenanger, Johannes, Hund, Martina, Strowitzki, Thomas, 2001. Relationship of seminal plasma interleukin (IL)-8 and IL-6 with semen quality. Hum. Reprod. 16 (3), 517–528.

Ellman, George L., 1959. Tissue sulfhydryl groups. Arch. Biochem. Biophys. 82 (1), 70–77.

Fanta, Duguma, Gebisa, Waqtola, Mamo, Aklilu, Tamiru, Dessalegn, Woyesa, Shiferaw, 2020. Diabetes mellitus and associated factors among adult HIV patients on highly active anti-retroviral treatment. HIV/AIDS (Auckland, NZ) 12, 657.

Fathi, Nasibeh, Hoseinipanah, Seyed Mohammad, Zohreh, Alizadeh, Assari, Mohammad Javad, Moghimbeigi, Abbas, Mortazavi, Motahare, Bahmanzadeh, Maryam, 2019. The effect of silver nanoparticles on the reproductive system of adult male rats: a morphological, histological and DNA integrity study. Adv. Clin. Exp. Med. 28 (3), 299–305.

Femi-Adepoju, Grace, Abiola, Dada, Oluwasogo, Adewumi, Otun, Kabir Opeyemi, Adepoju, Olufemi, Adeyinka, Fatoba, Ojo Paul, 2019. Green synthesis of silver nanoparticles using terrestrial fern (Gleichenia Pectinata (Willd.) C. Presl.): characterization and antimicrobial studies. Heliyon 5 (4), e01543.

Gagliardi, Mariacristina., 2017. Biomimetic and bioinspired nanoparticles for targeted drug delivery. Ther. Deliv. 8 (5), 289–299.

Galdiero, Stefania, Falanga, Annarita, Vitiello, Mariateresa, Cantisani, Marco, Marra, Veronica, Galdiero, Massimiliano, 2011. Silver nanoparticles as potential antiviral agents. Molecules 16 (10), 8894–8918.

Hakim, Zeenat S., Patel, Bhagirath K., Goyal, Ramesh K., 1997. Effects of chronic ramipril treatment in streptozotocin-induced diabetic rats. Indian J. Physiol. Pharmacol. 41 (4), 353–360.

Hedger, Mark P., Meinhardt, Andreas, 2003. Cytokines and the immune-testicular axis. J. Reprod. Immunol. 58 (1), 1–26.

Iacob, Iacob, Diana, G., Jugulete, Gheorghita, 2017. Improving the adherence to antiretroviral therapy, a difficult but essential task for a successful hiv treatment—clinical points of view and practical considerations. Front. Pharmacol. 8, 831.

Ismail, Onanuga O., Isaac, Jegede A., Ugochukwu, Offor, Oluwatosin, Ogedengbe, O., Aniekan, Peter I., Edwin, Naidu CS., Onyemaechi, Azu O., 2017. Impaired expression of testicular androgen receptor and collagen fibers in the testis of diabetic rats under HAART: the role of Hypoxis hemerocallidea. Folia Histochem. Cytobiol. 55 (3), 149–158.

Jyoti, K., Baunthiyal, M., Singh, A., 2016. Characterization of silver nanoparticles synthesized using Urtica dioica Linn. leaves and their synergistic effects with antibiotics. J. Radiat. Res. Appl. Sci. 9 (3), 217–227.

Kakkar, Poonam, Das, Ballabh, Viswanathan, P.N., 1984. A Modified Spectrophotometric Assay of Superoxide Dismutase.

Karpinski, Hauber, Ilona, Chemnitz, Jan, Schäfer, Paszkowski-Rogacz, Carola, Maciej, Chakraborty, Deboyoti, Grundhoff, Adam, 2016. Directed evolution of a recombinase that excises the provirus of most HIV-1 primary isolates with high specificity. Nat. Biotechnol. 34 (4), 401–409.

Kis, Robillard, Kevin, Chan, Gary, N.Y., Bendayan, Reina, 2010. The complexities of antiretroviral drug–drug interactions: role of ABC and SLC transporters. Trends Pharmacol. Sci. 31 (1), 22–35.

Kolb, H., Mandrup-Poulsen, T., 2005. An immune origin of type 2 diabetes? Diabetologia 48 (6), 1038–1050.

Lanning, Lynda L., Creasy, Dianne M., Chapin, Robert E., Mann, Peter C., Barlow, Norman, J., Regan, Karen, S., Goodman, Dawn G., 2002. Recommended approaches for the evaluation of testicular and epididymal toxicity. Toxicol. Pathol. 30 (4), 507–520.

Lara, Ixtepan-Turrent, Liliana, Garza-Treviño, Elsa, N., Rodriguez-Padilla, Cristina, 2010a. PVP-coated silver nanoparticles block the transmission of cell-free and cell-associated HIV-1 in human cervical culture. J. Nanobiotechnol. 8 (1), 15.

Lara, Humberto H., Ayala-Nuñez, Nilda, V., Ixtepan-Turrent, Liliana, Rodriguez-Padilla, Cristina, 2010b. Mode of antiviral action of silver nanoparticles against HIV-1. J. Nanobiotechnol. 8 (1), 1–10.

Lara, Humberto H., Ayala-Núñez, Nilda, V., Turrent, Liliana del, Carmen Ixtepan, Padilla, Cristina Rodríguez, 2010c. Bactericidal effect of silver nanoparticles against multidrug-resistant bacteria. World J. Microbiol. Biotechnol. 26 (4), 615–621.

Lawal, Sodiq Kolawole, Olojede, Samuel Oluwaseun, Dare, Ayobami, Faborode, Oluwaseun Samuel, Naidu Edwin Coleridge, S., Rennie, Carmen Olivia, Azu, Onyemaechi Okpara, 2021. Silver nanoparticles conjugate attenuates highly active antiretroviral therapy-induced hippocampal nissl substance and cognitive deficits in diabetic rats. J. Diabetes Res. 2021, 2118538.

Lee, Sang Hun, Jun, Bong-Hyun, 2019. Silver nanoparticles: synthesis and application for nanomedicine. Int. J. Mol. Sci. 20 (4), 865.

Long, Qiu, Cai, Han, Chen, Bing, Ningning, Lu, Xiaofang, Zheng, Shuhui, Li, Yubin, 2018. Hyperglycemia induced testicular damage in type 2 diabetes mellitus rats exhibiting microcirculation impairments associated with vascular endothelial growth factor decreased via PI3K/Akt pathway. Oncotarget 9 (4), 5321.

Mahajan, Aalinkeel, Ravikumar, Law, Wing-Cheung, Reynolds, Jessica, L., Nair, Bindukumar B., Sykes, Donald E., Schwartz, Stanley, A., 2012. Anti-HIV-1 nanotherapeutics: promises and challenges for the future. Int. J. Nanomed. 7, 5301.

Maritim, A.C., Sanders, aRA., Watkins Iii, J.B., 2003. Diabetes, oxidative stress, and antioxidants: a review. J. Biochem. Mol. Toxicol. 17 (1), 24–38.

Mzingwane, Mayibongwe L., Tiemessen, Caroline T., 2017. Mechanisms of HIV persistence in HIV reservoirs. Rev. Med. Virol. 27 (2), e1924.

Naidu, Edwin Coleridge S., Olojede, Samuel Oluwaseun, Lawal, Sodiq Kolawole, Rennie, Olivia, Carmen, Azu, Onyemaechi Okpara, 2021. Nanoparticle delivery system, highly active antiretroviral therapy, and testicular morphology: the role of stereology. Pharmacol. Res. Perspect. 9 (3), e00776.

Nair, Jacob, Shery, 2016. A simple practice guide for dose conversion between animals and human. J. Basic Clin. Pharm. 7 (2), 27.

Ogedengbe, Oluwatosin O., Jegede, Ayoob I., Onanuga, Ismail, O., Offor, Ugochukwu, Naidu, Edwin, C.S., Peter, Aniekan I., Azu, Onyemaechi O., 2016. Coconut oil extract mitigates testicular injury following adjuvant treatment with antiretroviral drugs. Toxicol. Res. 32 (4), 317–325.

Ohkawa, Hiroshi, Ohishi, Nobuko, Yagi, Kunio, 1979. Assay for lipid peroxides in animal tissues by thiobarbituric acid reaction. Anal. Biochem. 95 (2), 351–358.

Olasile, Ismail Onanuga, Jegede, I Ayoola, Offor, Ugochukwu, Ogedengbe, O Oluwatosin, Naidu, Edwin, C.S., Peter, I Aniekan, Azu, Onyemaechi O., 2018. Histo-morphological and seminal evaluation of testicular parameters in diabetic rats under antiretroviral therapy: interactions with Hypoxis hemerocallidea. Iran. J. Basic Med. Sci. 21 (12), 1322.

Osuji, Faustina, Nkechi, Onyenekwe, Chinedu, Charles, Ahaneku, Joseph, Ebere, Ukibe, Nkiruka Rose, 2018. The effects of highly active antiretroviral therapy on the serum levels of pro-inflammatory and anti-inflammatory cytokines in HIV infected subjects. J. Biomed. Sci. 25 (1), 1–8.

Oyeyipo, Ibukun, P., Skosana, Bongekile T., Everson, Frans P., Strijdom, Hans, Du, Plessis, Stefan, S., 2018. Highly active antiretroviral therapy alters sperm parameters and testicular antioxidant status in diet-induced obese rats. Toxicol. Res. 34 (1), 41–48.

Pace, Agosto, Luis, Graf, Erin, H., O'Doherty, Una, 2011. HIV reservoirs and latency models. Virology 411 (2), 344–354.

Patra, Jayanta Kumar, Gitishree Fraceto, Das, Fernandes, Leonardo, Campos, Estefania Vangelie Ramos, del Pilar Rodriguez-Torres, Maria, Acosta-Torres, Susana, Laura,

Sharma, Shivesh, 2018. Nano based drug delivery systems: recent developments and future prospects. J. Nanobiotechnol. 16 (1), 1–33.

Pilatz, A., Hudemann, C., Wagenlehner, F., Schuppe, H.C., Diemer, T., Weidner, W., Bschleipfer, T., 2013. Seminal cytokines: is quantification useful in urogenital disorders? Urol. Ausg. A 52 (3), 359–366.

Prabhu, Sathya, Vinodhini, Shanmugam, Elanchezhiyan, Chakravarthy, Rajeswari, Devi, 2018. Retracted: evaluation of antidiabetic activity of biologically synthesized silver nanoparticles using Pouteria sapota in streptozotocin-induced diabetic rats. J. Diabetes 10 (1), 28–42.

Pradhan, Deepak, Biswasroy, Prativa, Goyal, Amit, Ghosh, Goutam, Rath, Goutam, 2021. Recent advancement in nanotechnology-based drug delivery system Against viral infections. AAPS PharmSciTech 22 (1), 1–19.

Ramalho-Santos, Joao, Sandra, Amaral, Oliveira, Paulo J., 2008. Diabetes and the impairment of reproductive function: possible role of mitochondria and reactive oxygen species. Curr. Diabetes Rev. 4 (1), 46–54.

Ramamurthy, C.H., Padma, M., Mareeswaran, R., Suyavaran, A., Kumar, M Suresh, Premkumar, K., Thirunavukkarasu, C., 2013. The extra cellular synthesis of gold and silver nanoparticles and their free radical scavenging and antibacterial properties. Colloids Surf. B Biointerfaces 102, 808–815.

Rashid, Kahkashan, Sil, Parames C., 2015. Curcumin enhances recovery of pancreatic islets from cellular stress induced inflammation and apoptosis in diabetic rats. Toxicol. Appl. Pharmacol. 282 (3), 297–310.

Reigner, Blesch, Karen, 2002. Estimating the starting dose for entry into humans: principles and practice. Eur. J. Clin. Pharmacol. 57 (12), 835–845.

Ricci, G., Catizone, A., Esposito, R., Pisanti, F.A., Vietri, M.T., Galdieri, M., 2009. Diabetic rat testes: morphological and functional alterations. Andrologia 41 (6), 361–368.

Rodger, Alison J., Fox, Zoe, Lundgren, Jens, D., Kuller, Lewis, H., Boesecke, Christoph, Gey, Daniela, Group, INSIGHT Strategies for Management of Antiretroviral Therapy Study, 2009. Activation and coagulation biomarkers are independent predictors of the development of opportunistic disease in patients with HIV infection. J. Infect. Dis. 200 (6), 973–983.

Romano, R.M., Romano, M.A., Bernardi, M.M., Furtado, P.V., Oliveira, C.A., 2010. Prepubertal exposure to commercial formulation of the herbicide glyphosate alters testosterone levels and testicular morphology. Arch. Toxicol. 84 (4), 309–317.

Rose-John, Stefan., 2018. Interleukin-6 family cytokines. Cold Spring Harb. Perspect. Biol. 10 (2), a028415.

Rossetti, Luciano, DeFronzo, Ralph A., Gherzi, Roberto, Stein, Peter, Andraghetti, Gabriella, Falzetti, Giorgio, Cordera, Renzo, 1990. Effect of metformin treatment on insulin action in diabetic rats: in vivo and in vitro correlations. Metabolism 39 (4), 425–435.

Saratale, Ganesh Dattatraya, Saratale, Rijuta Ganesh, Benelli, Giovanni, Kumar, Gopalakrishnan, Pugazhendhi, Arivalagan, Kim, Dong-Su, Shin, Han-Seung, 2017. Anti-diabetic potential of silver nanoparticles synthesized with Argyreia nervosa leaf extract high synergistic antibacterial activity with standard antibiotics against foodborne bacteria. J. Cluster Sci. 28 (3), 1709–1727.

Savasi, Oneta, Monica, Laoreti, Arianna, Parisi, Francesca, Parrilla, Bina, Duca, Piergiorgio, Cetin, Irene, 2018. Effects of antiretroviral therapy on sperm DNA integrity of HIV-1-infected men. Am. J. Men's Health 12 (6), 1835–1842.

Siddiqi, Khwaja Salahuddin, Husen, Azamal, Rao, Rifaqat A.K., 2018. A review on biosynthesis of silver nanoparticles and their biocidal properties. J. Nanobiotechnol. 16 (1), 14.

Sinha, Rajni, Kim, Gloria J., Nie, Shuming, Shin, Dong M., 2006. Nanotechnology in cancer therapeutics: bioconjugated nanoparticles for drug delivery. Mol. Cancer Therapeut. 5 (8), 1909–1917.

Turkevich, John, Stevenson, Peter Cooper, Hillier, James, 1951. A study of the nucleation and growth processes in the synthesis of colloidal gold. Discuss. Faraday Soc. 11, 55–75.

van Leeuwen, Elisabeth, Wit, Ferdinand, W., Repping, Sjoerd, Schattenkerk, M Eeftinck, Jan Karel, Reiss, Peter, van der Veen, Fulco, Prins, Jan M., 2008. Effects of antiretroviral therapy on semen quality. AIDS 22 (5), 637–642.

Verweel, Gwenda, van Rossum, Annemarie, M.C., Hartwig, Nico G., Wolfs, Tom, F.W., Scherpbier, Henriëtte, J., de Groot, Ronald, 2002. Treatment with highly active antiretroviral therapy in human immunodeficiency virus type 1-infected children is associated with a sustained effect on growth. Pediatrics 109 (2), e25.

Wilson, Islam, Md Shahidul, 2012. Fructose-fed streptozotocin-injected rat: an alternative model for type 2 diabetes. Pharmacol. Rep. 64 (1), 129–139.

Yerragopu, Prem Santhi, Hiregoudar, Sharanagouda, Nidoni, Udaykumar, Ramappa, K.T., Sreenivas, A.G., Doddagoudar, S.R., 2020. Chemical synthesis of silver nanoparticles using tri-sodium citrate, stability study and their characterization. Int. Res. J. Pure Appl. Chem. 37–50.

Yilma, Abebayehu N., Singh, Shree R., Dixit, Saurabh, Dennis, Vida A., 2013. Anti-inflammatory effects of silver-polyvinyl pyrrolidone (Ag-PVP) nanoparticles in mouse macrophages infected with live Chlamydia trachomatis. Int. J. Nanomed. 8, 2421.

Zhang, Liu, Zhi-Guo, Shen, Wei, Gurunathan, Sangiliyandi, 2016. Silver nanoparticles: synthesis, characterization, properties, applications, and therapeutic approaches. Int. J. Mol. Sci. 17 (9), 1534.